Multi-leg NLO

Ansgar Denner, PSI (still)

QCD at the LHC, Trento, September 26 – October 1, 2010

- Short description of Feynman diagrammatic methods using $\mathrm{p\bar{p}} \to \mathrm{t\bar{t}b\bar{b}}$ as example
- Some numerical results for $\mathrm{p\bar{p}} \to \mathrm{t\bar{t}b\bar{b}}$

$2 \rightarrow 4$ processes of Les Houches 2005/2007 priority list

Big progress during last 2 years

reaction	existing calculations	method
$\mathrm{pp} \rightarrow \mathrm{t\bar{t}b\bar{b}}$	Bredenstein, Denner, Dittmaier, Pozzorini '09	Feynman diagrams
	Bevilacqua, Czakon, Papadopoulos, Pittau, Worek '09	OPP reduction and HELAC
$\mathrm{pp} \rightarrow \mathrm{t\bar{t}}jj$	Bevilacqua, Czakon, Papadopoulos, Worek '10	OPP reduction and HELAC
$\mathrm{pp} \rightarrow VV\mathrm{b\bar{b}}$	–	
$\mathrm{pp} \rightarrow VVjj$	Melia, Melnikov, Röntsch, Zanderighi '10 $(\mathrm{W^+W^+})$	D-dimensional unitarity
$\mathrm{pp} \rightarrow Vjjj$	Berger et al. '09 (W)	generalised unitarity
	R.K.Ellis et al. '09 (W, leading colour)	D-dimensional unitarity
	Berger et al. '10 (Z)	generalised unitarity
$\mathrm{pp} \rightarrow \mathrm{b\bar{b}b\bar{b}}$	Binoth et al. '09 ($q\bar{q}$ channel)	Feynman diagrams

virtual amplitudes for all these $2 \rightarrow 4$ processes: van Hameren, Papadopoulos, Pittau '09

first $2 \rightarrow 5$ process: $\mathrm{pp} \rightarrow \mathrm{W}jjjj$ Berger et al. arXiv:1009.2338 generalised unitarity

Feynman-diagrammatic methods

consider only Feynman-diagrammatic methods in this talk

active groups/people

- GOLEM: Binoth, Guffanti, Guillet, Heinrich, Karg, Kauer, Reiter, Sanguinetti
- Bredenstein, Denner, Dittmaier, Pozzorini, Kallweit, ...
- GRACE: Boudjema, Fujimoto, Ishikawa, Kaneko, Kurihara, Shimizu, Kato, Yasui
- chinese group(s): Guo, Ma, Wang, Zhang... (mainly ILC processes)

explain our (Denner/Dittmaier) methods using $\mathrm{pp} \to \mathrm{t\bar{t}b\bar{b}}$ as example

methods of other groups different in detail

Contributions to $t\bar{t}b\bar{b}$ at NLO

Partonic channels

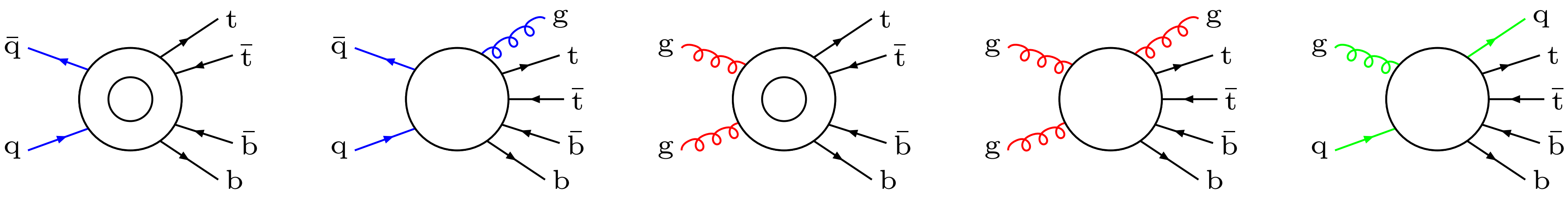

Relative weights and number of Feynman diagrams channels

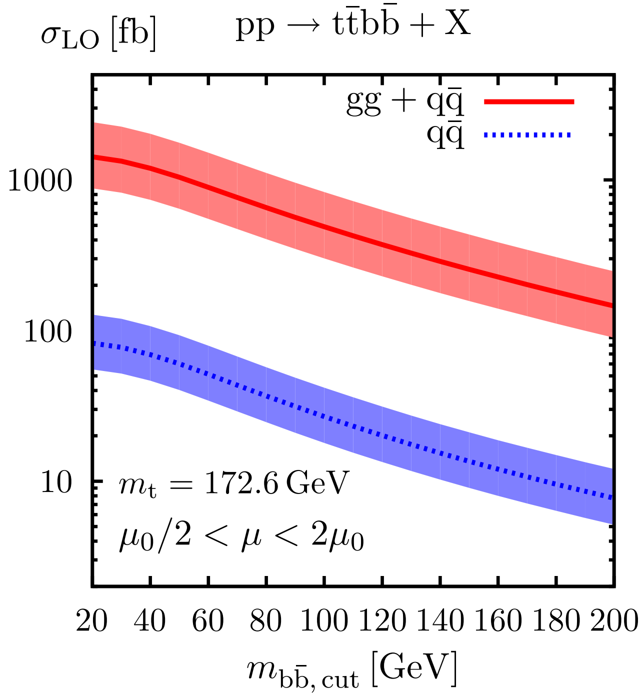

	$q\bar{q}$	gg	qg
# of LO diags	7	36	
# of virtual diags	188	1003	
# of real diags	64	341	64
$(\sigma/\sigma_{tot})_{LO}$	5%	95%	
$(\sigma/\sigma_{tot})_{NLO}$	3%	92%	5%

Tree and one-loop contributions to $\mathrm{pp} \to \mathrm{t\bar{t}b\bar{b}} + X$

Tree and one-loop diagrams in $q\bar{q}$ and gg channels

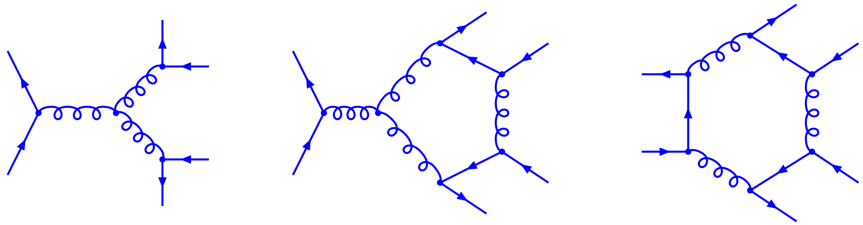

7 trees | 24 pentagons | 8 hexagons

188 loops

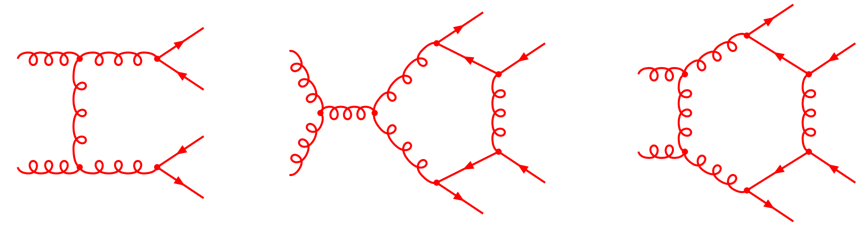

36 trees | 114 pentagons | 40 hexagons

1003 loops

two independent calculations

- generation of diagrams with FeynArts 1.0 and 3.2 Küblbeck et al. '90,'92; Hahn '01
- algebraic simplifications using two independent in-house programs implemented in *Mathematica*, one using FormCalc 5.2 Hahn '06 for preliminary algebraic manipulations (Dirac algebra, covariant decomposition)
- reduction of tensor integrals according to

  Denner, Dittmaier, NPB658 (2003)175 [hep-ph/0212259], NPB734 (2006) 62 [hep-ph/0509141]

  $\hookrightarrow$ numerically stable results (two libraries for tensor integrals)

top quarks massive and bottom quarks massless

Structure of one-loop contributions to $\mathrm{pp} \longrightarrow \mathrm{t\bar{t}b\bar{b}} + X$

Structure of typical individual diagram:

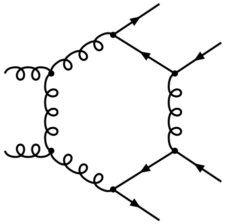

$$f^{a_1bd}f^{a_2cd}(T^bT^e)_{i_3i_4}(T^cT^e)_{i_5i_6} \times \sum a_{k_1\ldots k_P}$$

$$\varepsilon_{\mu_1}\varepsilon_{\mu_2}[\bar{v}_3\gamma_{\mu_3}\ldots u_4][\bar{v}_5\ldots\gamma_{\mu_k}\ldots u_6]\{g\ldots p\}^{\mu_1\ldots\nu_P}_{k_1\ldots k_p}\int \mathrm{d}^Dq\frac{q_{\nu_1}\ldots q_{\nu_P}}{N_0\ldots N_{N-1}}$$

$\Rightarrow$ decomposition of individual diagram

$$\mathcal{M}^{(\Gamma)} = \underbrace{\mathcal{C}^{(\Gamma)}}_{\substack{\text{factorized}\\ \text{colour structure}}} \sum_m \mathcal{F}_m^{(\Gamma)}(\{p_a\cdot p_b\})\underbrace{\hat{\mathcal{M}}_m(\{p_a\},\{\lambda\})}_{\substack{\text{standard matrix}\\ \text{elements}}}$$

invariant functions $\mathcal{F}_m^{(\Gamma)}$

$$\mathcal{F}_m^{(\Gamma)}(\{p_a\cdot p_b\}) = \sum_{j_1\cdots j_R}\mathcal{K}^{(\Gamma)}_{m,j_1\ldots j_R}(\{p_a\cdot p_b\})\underbrace{T_{j_1\ldots j_R}(\{p_a\cdot p_b\})}_{\text{tensor loop coefficients}}$$

computed numerically diagram by diagram

many common substructures are recycled in the numerical calculation (tensor integrals, helicity amplitudes)

Treatment of colour

Colour structure factorizes for individual diagrams Γ

$$\mathcal{M}^{(\Gamma)} = \underbrace{\mathcal{C}^{(\Gamma)}}_{\substack{\text{factorized}\\ \text{colour structure}}} \sum_m \underbrace{\mathcal{F}_m^{(\Gamma)}(\{(p_a p_b)\})}_{\substack{\text{invariant}\\ \text{functions}}} \underbrace{\hat{\mathcal{M}}_m(\{p_a\},\{\lambda\})}_{\substack{\text{standard matrix}\\ \text{elements}}}$$

colour structure decomposed in suitable basis: $\mathcal{C}^{(\Gamma)} = \sum_k a_k \mathcal{C}_k^{(\Gamma)}$

- $\bar{\mathrm{q}}\mathrm{q} \to \mathrm{t}\bar{\mathrm{t}}\mathrm{b}\bar{\mathrm{b}}$: six colour structures

$$1 \otimes 1 \otimes 1 \quad f^{abc} T^a \otimes T^b \otimes T^c, \quad d^{abc} T^a \otimes T^b \otimes T^c, \quad 1 \otimes T^a \otimes T^a, \quad \ldots$$

- $\mathrm{gg} \to \mathrm{t}\bar{\mathrm{t}}\mathrm{b}\bar{\mathrm{b}}$: 14 colour structures

$$\delta^{ab}\, 1 \otimes 1, \quad T^a \otimes T^b, \quad f^{abc}\, 1 \otimes T^c, \quad d^{abc}\, 1 \otimes T^c, \quad f^{ach} f^{bdh}\, T^b \otimes T^c, \ldots$$

- only one colour structure for most diagrams
  only a few for other diagrams
  factor 3 for each $4\mathrm{g}$ vertex: $f^{abh} f^{cdh} (g_{\mu\nu} g_{\rho\sigma} - g_{\mu\sigma} g_{\rho\nu}) + 2\ \mathrm{perm.}$
  $\Rightarrow$ CPU time does not scale with number of colour factors

Reduction of standard matrix elements for $\bar{q}q \to t\bar{t}b\bar{b}$

structure of standard matrix elements (SMEs)

$$\underbrace{\bar{v}(p_1)\ldots\gamma^\mu\gamma^\nu\not{p}_3\ldots u(p_2)}_{q\bar{q}\text{ chain}}\;\underbrace{\bar{v}(p_3)\ldots\gamma^\mu\gamma^\nu\gamma^\rho\not{p}_6\ldots u(p_4)}_{t\bar{t}\text{ chain}}\;\underbrace{\bar{v}(p_5)\ldots\gamma^\rho\not{p}_2\not{p}_3\ldots u(p_6)}_{b\bar{b}\text{ chain}}$$

process-independent identities in D dimensions

- Dirac equation, Dirac algebra, momentum conservation, standard ordering
  $\Rightarrow \mathcal{O}(10^3)$ Dirac structures, still many $\gamma^\mu \otimes \gamma_\mu$ contractions between chains

after cancellation of $1/(D-4)$ poles use identities in 4 dimensions

- introduce chiral projectors $\omega_\pm = \frac{1}{2}(1 \pm \gamma_5)$ via $u(p_j) \Rightarrow [\omega_+ + \omega_-]u(p_j)$
  and exploit identities of type $\gamma^\mu\gamma^\alpha\gamma^\beta\omega_\pm \otimes \gamma_\mu\omega_\mp = \gamma^\mu\omega_\pm \otimes \gamma^\alpha\gamma^\beta\gamma_\mu\omega_\mp$
  to exchange Dirac matrices between different Dirac chains

construct a sophisticated, process-dependent algorithm

$\Rightarrow$ reduction of all Dirac structures to ~ 200 SMEs

without introducing new denominators that might spoil numerical stability

Reduction of standard matrix elements for $\mathrm{gg} \to \mathrm{t\bar{t}b\bar{b}}$

structure of standard matrix elements (SMEs)

$$\underbrace{\{\epsilon_1^\mu \epsilon_2^\nu, (\epsilon_1\epsilon_2)p_2^\mu p_4^\nu, (\epsilon_1 p_4)(\epsilon_2 p_3)g^{\mu\nu}, \ldots\}}_{\text{gluon polarization vectors}} \underbrace{\bar{v}(p_3)\ldots\gamma^\mu\gamma^\rho \not{p}_6 \ldots u(p_4)}_{\mathrm{t\bar{t}}\text{ chain}} \underbrace{\bar{v}(p_5)\ldots\gamma^\nu\gamma^\rho \not{p}_2 \ldots u(p_6)}_{\mathrm{b\bar{b}}\text{ chain}}$$

process-independent identities in D dimensions

- $\epsilon_i p_i = 0$, Dirac eq., Dirac algebra, momentum conservation, standard ordering

two alternative reductions in $D = 4$

- sophisticated method similarly as for $q\bar{q}$ channel $\Rightarrow$ 502 SMEs
- less sophisticated and process-independent reduction based only on

$$\gamma^{\mu_1}\gamma^{\mu_2}\gamma^{\mu_3}\gamma^{\mu_4}\gamma^{\mu_5} = g^{\mu_1\mu_2}\gamma^{\mu_3}\gamma^{\mu_4}\gamma^{\mu_5} + \ldots + g^{\mu_1\mu_2}g^{\mu_3\mu_4}\gamma^{\mu_5} + \ldots$$

$\Rightarrow$ 970 SMEs

result: speed of codes based on both reductions almost identical

$\Rightarrow$ sophisticated process-dependent manipulations not needed for this process

Rational terms from dimensional regularization

Rational terms originate from $1/(D-4)$ poles of tensor loop integrals

rational terms of UV origin easily obtained via

$$\mathcal{K}^{(\Gamma)}_{m,j_1\ldots j_R}(D)\ \underbrace{T_{j_1\ldots j_R}}_{\frac{R_{j_1\cdots j_R}}{(D-4)}+T^{\mathrm{finite}}_{j_1\cdots j_R}} = \mathcal{K}^{(\Gamma)}_{m,j_1\ldots j_R}(4)\,T_{j_1\ldots j_R} + \mathcal{K}'^{(\Gamma)}_{m,j_1\ldots j_R}(4)\,R_{j_1\ldots j_R} + \mathcal{O}(D-4)$$

- UV residues $R_{j_1\ldots j_R}$ of tensor integrals explicitly available
- easily included in algebraic reduction

rational terms of IR origin arise from double and single IR poles of loop integrals

$$\mathcal{K}_{j_1\ldots j_R}(D)\ \underbrace{T_{j_1\ldots j_R}}_{\frac{R_{2;j_1\cdots j_R}}{(D-4)^2}+\frac{R_{1;j_1\cdots j_R}}{(D-4)}+\mathrm{IR{-}finite\,part}} \Rightarrow \mathcal{K}'_{j_1\ldots j_R}(4)\,R_{1,j_1\ldots j_R} + \frac{1}{2}\mathcal{K}''_{j_1\ldots j_R}(4)\,R_{2,j_1\ldots j_R} + \ldots$$

- can require lot of algebraic work (second-order expansion, many contributions)
- cancel completely in truncated (!) one-loop amplitudes $\Rightarrow$ omit from the start

  Bredenstein, Denner, Dittmaier, Pozzorini ’08 [arXiv:0807.1248]

Cancellation of rational terms of IR origin (sketch of proof)

Rational terms originate from D-dependent $g^{\mu\nu}$ contractions of type $g_{\nu\lambda}\Gamma^{\nu\lambda}$

$$g_{\nu\lambda}g^{\nu\lambda} = D, \qquad g_{\nu\lambda}\gamma^{\nu}\not{p}\gamma^{\lambda} = (2-D)\not{p}, \qquad \ldots$$

- tensor reduction is free of IR rational terms, since soft and collinear singular tensor coefficients do not multiply $g^{\mu\nu}$ $\quad (q^{\mu} \to xp^{\mu})$
- in all possible diagrams involving IR-divergent integrals

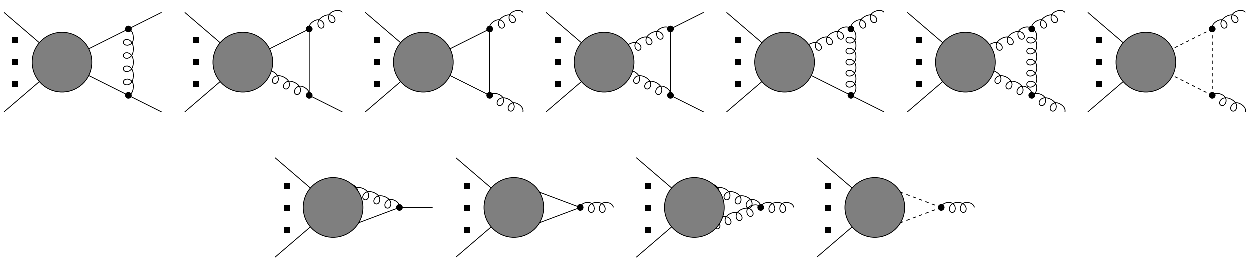

$g_{\nu\lambda}\Gamma^{\nu\lambda}$ contractions cancel in IR regions:

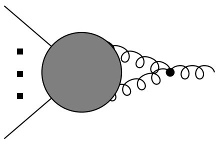

$$= \int \mathrm{d}^D q \, \frac{1}{q^2(q+p)^2} \underbrace{\varepsilon^{\mu *}(p)\,(2q+p)_{\mu}}_{\to 0 \text{ in soft/coll. regions}} \, g_{\nu\lambda}\Gamma^{\nu\lambda}(q) + \ldots$$

Algebraic reduction of tensor integrals

Methods developped for $\mathrm{e}^+\mathrm{e}^- \to 4f$ Denner, Dittmaier hep-ph/0509141

Avoid instabilities from small Gram determinants in denominators!

- 1- and 2-point integrals: numerically stable explicit expressions (no reduction)
- 3-point and 4-point integrals: reduction method depends on phase-space point (determined on the fly)
  - phase-space regions without Gram determinant instabilities: Passarino–Veltman reduction
  - otherwise, instabilities are avoided by various alternative reductions
    - −− expansions in small determinants (see also R.K.Ellis et al. ’05)
    - −− analytical special cases
    - −− semi-numerical method (see also Binoth et al. ’05; Ferroglia et al. ’02)
- for $N > 4$ use 4-dimensionality of space-time

  5-point integrals $\to$ five 4-point integrals Melrose ’65; Denner, Dittmaier ’02, ’05

  6-point integrals $\to$ six 5-point integrals (see also Binoth et al. ’05)

  without inverse Gram determinants and simultaneous reduction of rank by one

Algebraic reduction of tensor integrals II

Reduction of 3- and 4-point integrals

- reduction method selected on the fly
  depending on several estimates on numerical accuracy
- expansion in small determinants (fast)

  schematically: $D^{(P)} = C^{(P)} + \det(Z) D^{(P+1)}$

  iterative expansion with expansion depth K adapted to $\det(Z)$ and target precision

  $$D^{(P)} = D_K^{(P)} + \mathcal{O}(\det(Z)^{K+1}) \qquad \text{requires } D_0^{(P+K)} \text{ and } C^{(P+K)}$$

- semi-numerical method (similar methods used by GOLEM)
  numerical integration comparably slow
  typically used for checks only, not for production

methods developped for electroweak corrections to $\mathrm{e}^+\mathrm{e}^- \to 4f$
simply taken over for QCD corrections to $2 \to 4$ processes
NLO QCD correcctions seem to be not as tricky as electroweak corrections

Real corrections for $\mathrm{pp} \to \mathrm{t\bar{t}b\bar{b}} + X$

Diagrams and matrix elements

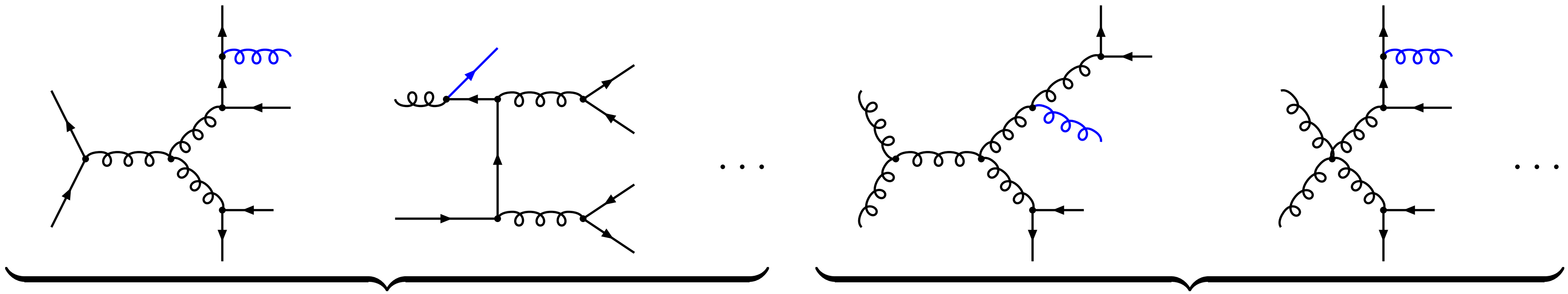

$\bar{\mathrm{q}}\mathrm{q} \to \mathrm{t\bar{t}b\bar{b}g}$ and $q\mathrm{g} \to \mathrm{t\bar{t}b\bar{b}}q$ (64 diagrams) $\mathrm{gg} \to \mathrm{t\bar{t}b\bar{b}g}$ (341 diagrams)

- with `Madgraph 4.1.33` Alwall et al. '07 for all channels
  analytically with Weyl–van der Waerden spinors Dittmaier '98 for $q\bar{q}/q\mathrm{g}$ channels
  numerically with off-shell recursion relations Berends, Giele '88, ... for gg channel

soft and collinear singularities

- regularized dimensionally or with infinitesimal gluon and quark masses
- dipole subtraction Catani, Seymour '96; Catani, Dittmaier, Seymour, Trócsányi '02
  30 subtraction terms for $q\bar{q}/\mathrm{gg}$ channels and 10 for $q\mathrm{g}$ channel
- initial-state collinear singularities cancelled by $\overline{\mathrm{MS}}$ redefinition of PDFs

phase-space integration

- adaptive multi-channel Monte Carlo Berends, Kleiss, Pittau '94; Kleiss, Pittau '94
  $\mathcal{O}(1400)$ channels to map all peaks from propagators (300) and dipoles (1100)

Confirmation by Bevilacqua et al.

Results have been confirmed at per-mille level

Bevilacqua et al., arXiv:0907.4723:

Process	$\sigma^{\text{LO}}_{\text{BDDP}}$ [fb]	$\sigma^{\text{LO}}_{\text{BCPPW}}$ [fb]	$\sigma^{\text{NLO}}_{\text{BDDP}}$ [fb]	$\sigma^{\text{NLO}}_{\text{BCPPW}\,\alpha_{max}=1}$ [fb]	$\sigma^{\text{NLO}}_{\text{BCPPW}\,\alpha_{max}=0.01}$ [fb]
$q\bar{q} \to t\bar{t}b\bar{b}$	85.522(26)	85.489(46)	87.698(56)	87.545(91)	87.581(134)
$pp \to t\bar{t}b\bar{b}$	1488.8(1.2)	1489.2(0.9)	2638(6)	2642(3)	2636(3)

Table 1: *Cross sections for $pp \to t\bar{t}b\bar{b} + X$ at the LHC at LO and NLO for the scale choice $\mu_F = \mu_R = m_t$, from* Bredenstein et al. *and* Bevilacqua et al.. *The statistical errors are quoted in parentheses.*

LO and NLO scale dependence for $pp \to t\bar{t}b\bar{b} + X$

Bredenstein, Denner, Dittmaier, Pozzorini
arXiv:0905.0110
LO, NLO: $\mu_F = \mu_R$
LO', NLO': $\mu_F = m_t^2/\mu_R$

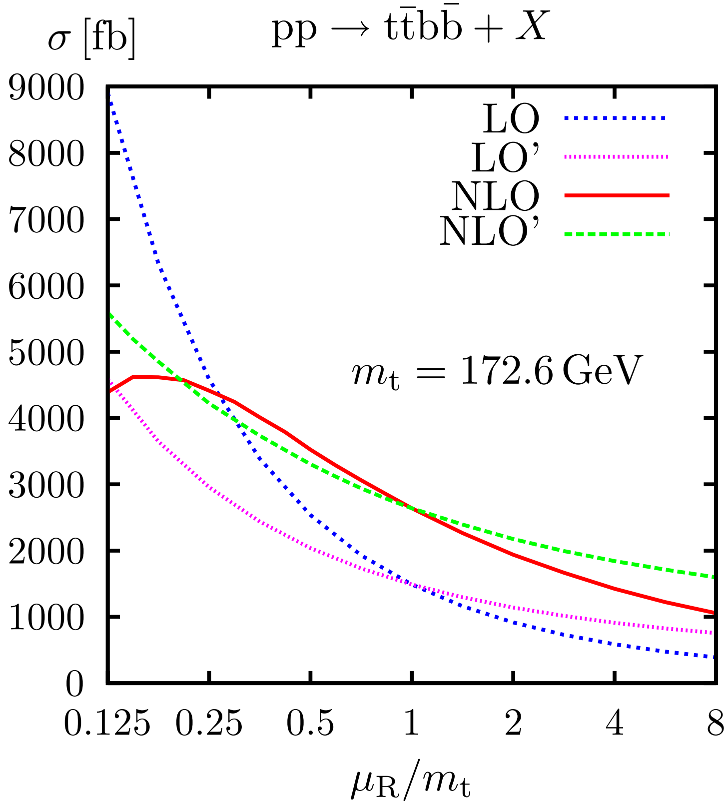

High sensitivity to scale choice

- LO proportional to $\alpha_S(\mu_R)^4$
  $\Rightarrow$ 70–80% scale uncertainty

original scale choice based on $t\bar{t}H$ ($K \simeq 1.2$)

$$\mu_0 = E_{thr}/2 = m_t + m_{b\bar{b}}/2$$

- used by ATLAS assuming $t\bar{t}b\bar{b} \simeq t\bar{t}H$
- yields large K factor (1.8) and scale dependence (34%) ($D = 0.8, m_{b\bar{b},cut} = 0$)

QCD dynamics of $t\bar{t}H$ and $t\bar{t}b\bar{b}$ different

- $(gg \to t\bar{t}H) \times (H \to b\bar{b}) = \mathcal{O}(\alpha_s^2)$
- $(gg \to t\bar{t}g) \times (g \to b\bar{b}) = \mathcal{O}(\alpha_s^4)$
- several different channels for $t\bar{t}b\bar{b}$
  $\Rightarrow$ no simple mechanism that fixes scale

Transverse momentum distributions for $\mathrm{pp} \to \mathrm{t\bar{t}b\bar{b}} + X$

Bredenstein, Denner, Dittmaier, Pozzorini

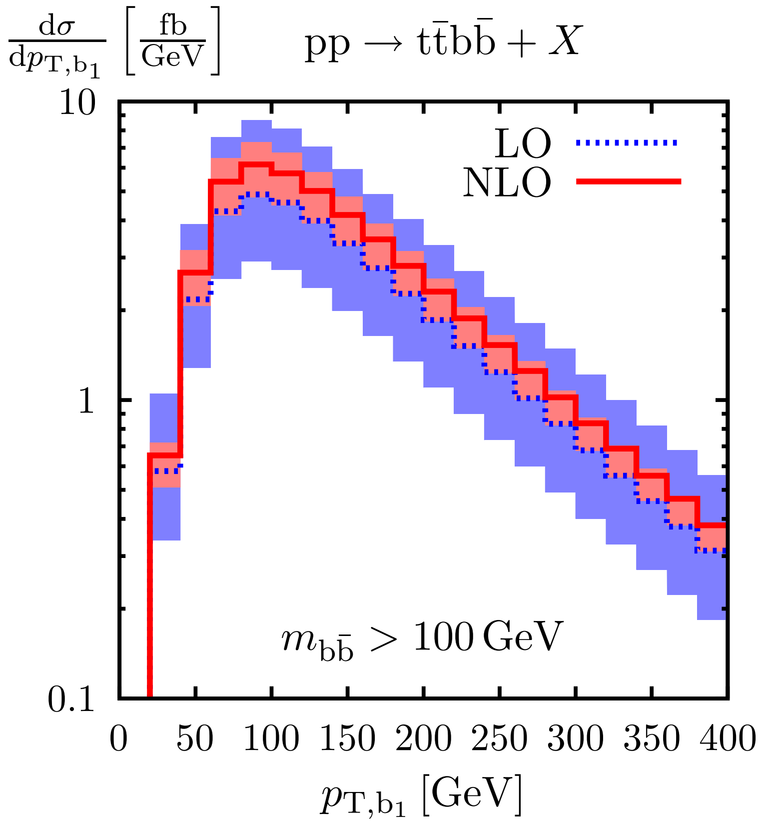

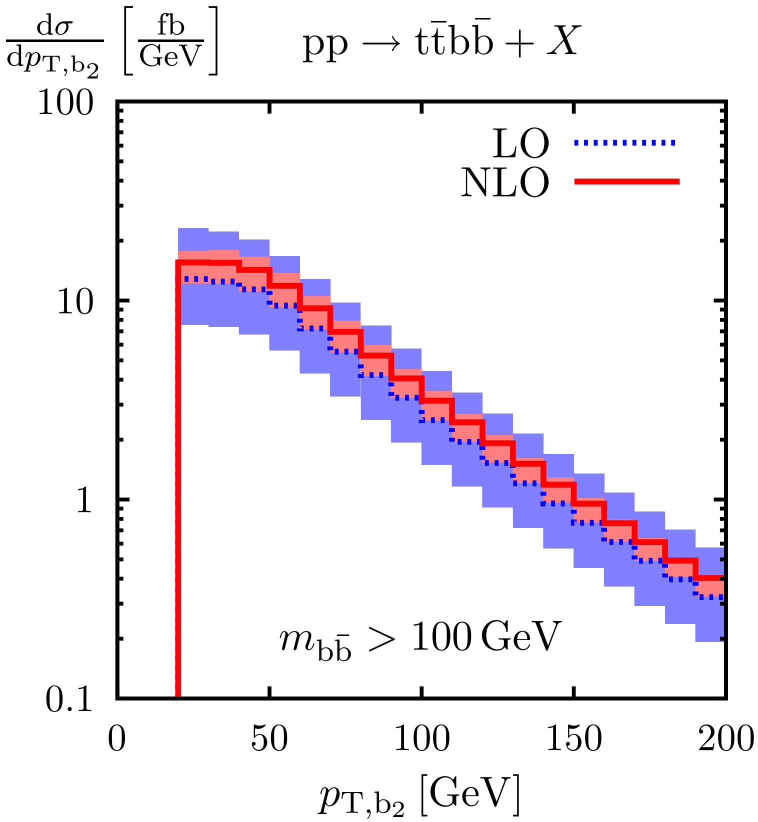

b-jets have typically $p_{T,b} \ll m_t$ and rather different distributions

- harder b jet (left) peaks at $p_{T,b} \sim 100\,\mathrm{GeV}$
- softer b jet (right) tends to saturate cut at $20\,\mathrm{GeV}$

introduce effective scale $\mu_0^2 = m_t \sqrt{p_{T,b} p_{T,\bar{b}}}$

Transverse momentum distributions for $pp \to t\bar{t}b\bar{b} + X$

Bredenstein, Denner, Dittmaier, Pozzorini

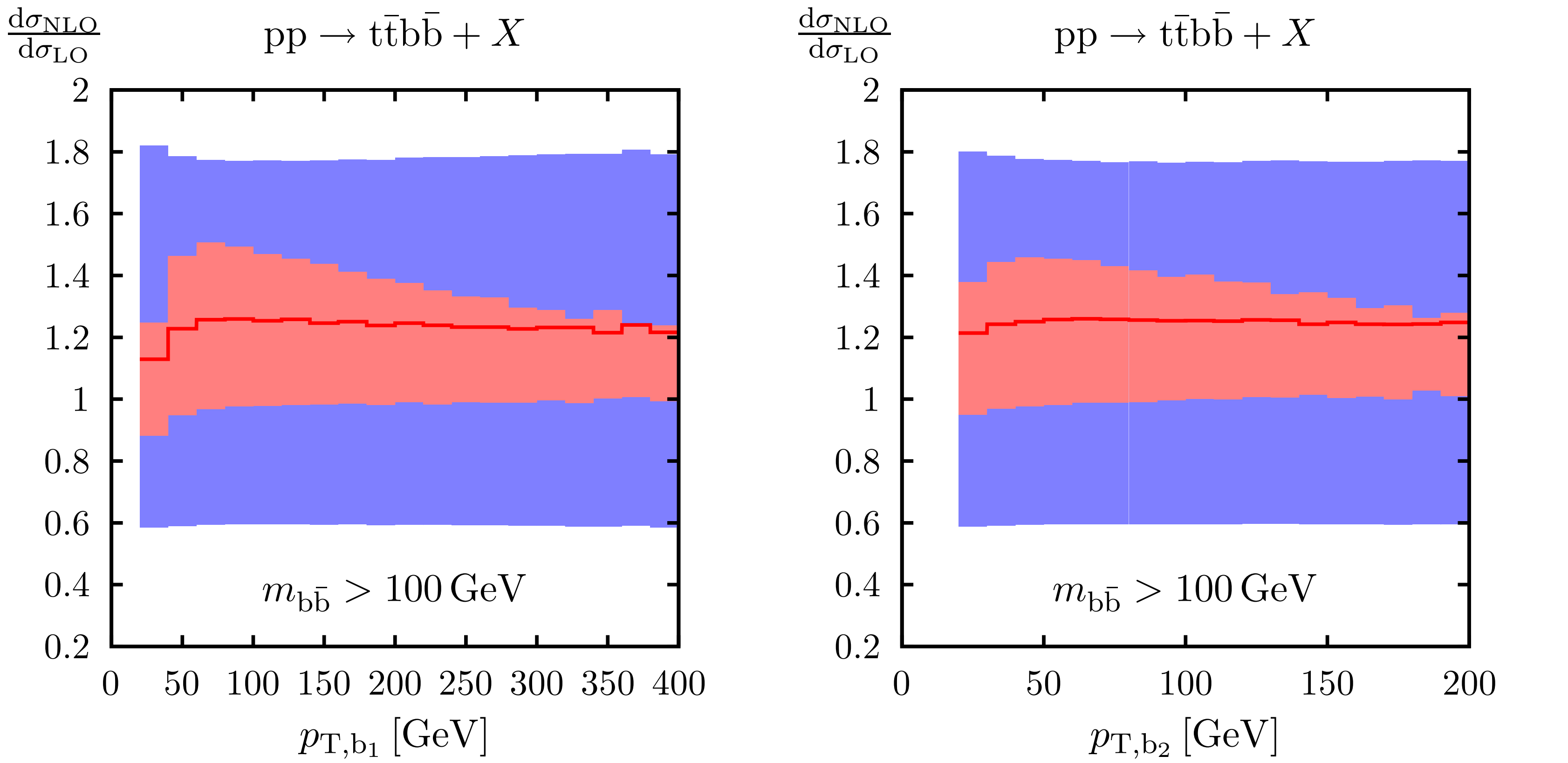

New scale choice improves convergence:

- NLO band perfectly fits within LO band: $K \simeq 1.25$
- K-factor almost constant over wide $p_{T,b}$ range for both b quarks
- NLO scale uncertainty reduced to about 20%

LO and NLO scale dependence for $\mathrm{pp} \to \mathrm{t\bar{t}b\bar{b}} + X$

Bredenstein, Denner, Dittmaier, Pozzorini

arXiv:1001.4006

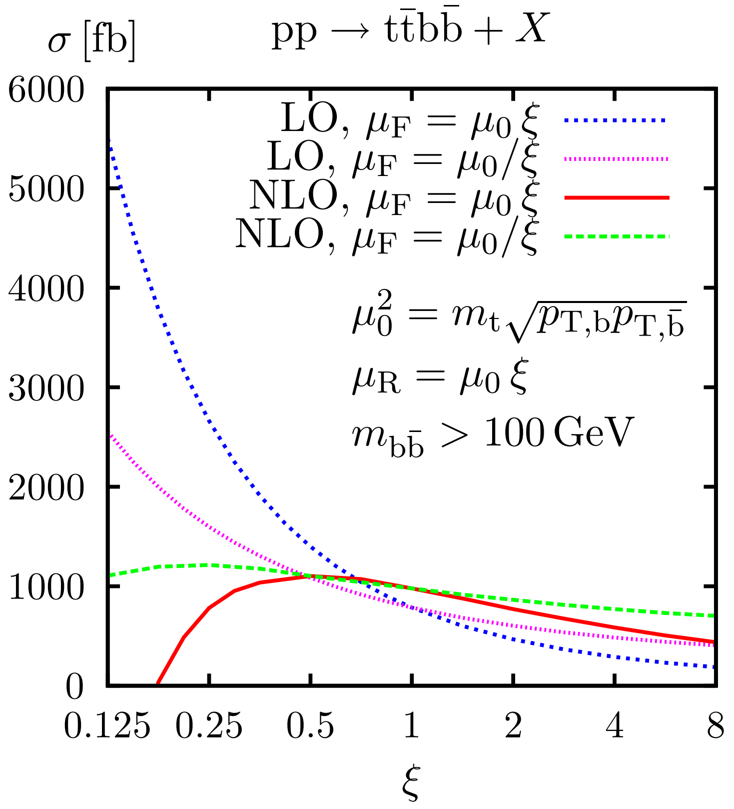

Variations around new central scale

$$\mu_0^2 = m_\mathrm{t}\sqrt{p_{\mathrm{T,b}}p_{\mathrm{T,\bar{b}}}}$$

good news for theory: improved convergence

- small correction and uncertainty:
  $K = 1.24 \pm 21\%$
- central scale close to a maximum

bad news for experiment:
enhancement of $\mathrm{t\bar{t}b\bar{b}}$ background

- already large for old scale $\mu_\mathrm{old} = E_\mathrm{thr}/2$:
  $K \simeq 1.8$
- even worse with new scale
  ($\sigma_\mathrm{NLO}(\mu_0)/\sigma_\mathrm{LO}(E_\mathrm{thr}/2) \simeq 2.18$)
  since $\mu_0 \simeq 0.5\mu_\mathrm{old}$
  (in spite of smaller K factor)

$\mathrm{b\bar{b}}$ invariant-mass distribution for $\mathrm{pp} \to \mathrm{t\bar{t}b\bar{b}} + X$

crucial observable for $\mathrm{t\bar{t}H}$ production

Bredenstein, Denner, Dittmaier, Pozzorini

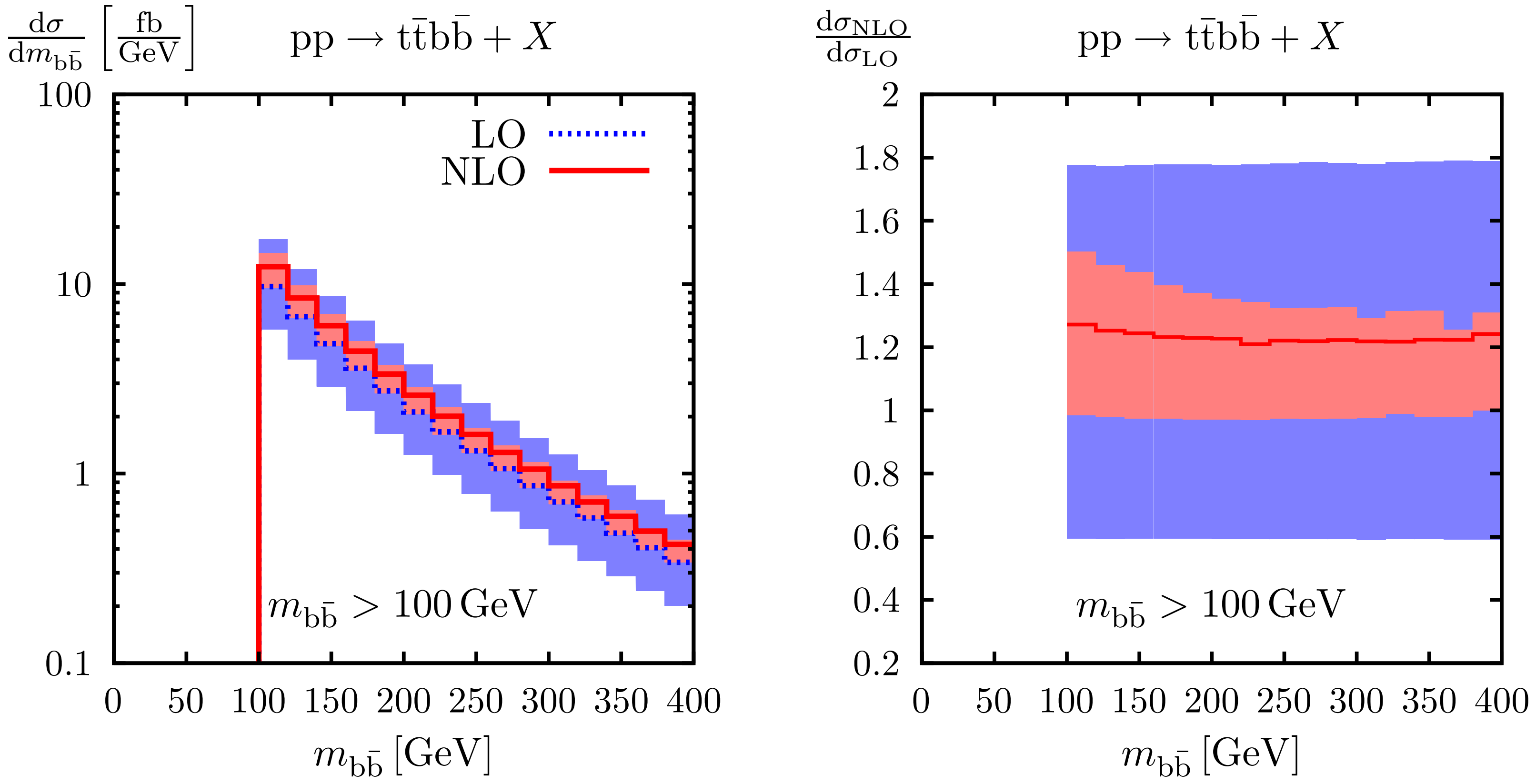

- small NLO correction $K \simeq 1.24$
- K-factor almost constant over wide $m_{\mathrm{b\bar{b}}}$ range
- NLO scale uncertainty $\sim 20\%$

$\mathrm{b\bar{b}}$ invariant-mass distribution for $\mathrm{pp} \to \mathrm{t\bar{t}b\bar{b}} + X$

Setup with highly boosted $\mathrm{b\bar{b}}$ pairs: $p_{\mathrm{T,b\bar{b}}} > 200\,\mathrm{GeV}$ (instead of $m_{\mathrm{b\bar{b}}} > 100\,\mathrm{GeV}$)

Bredenstein, Denner, Dittmaier, Pozzorini

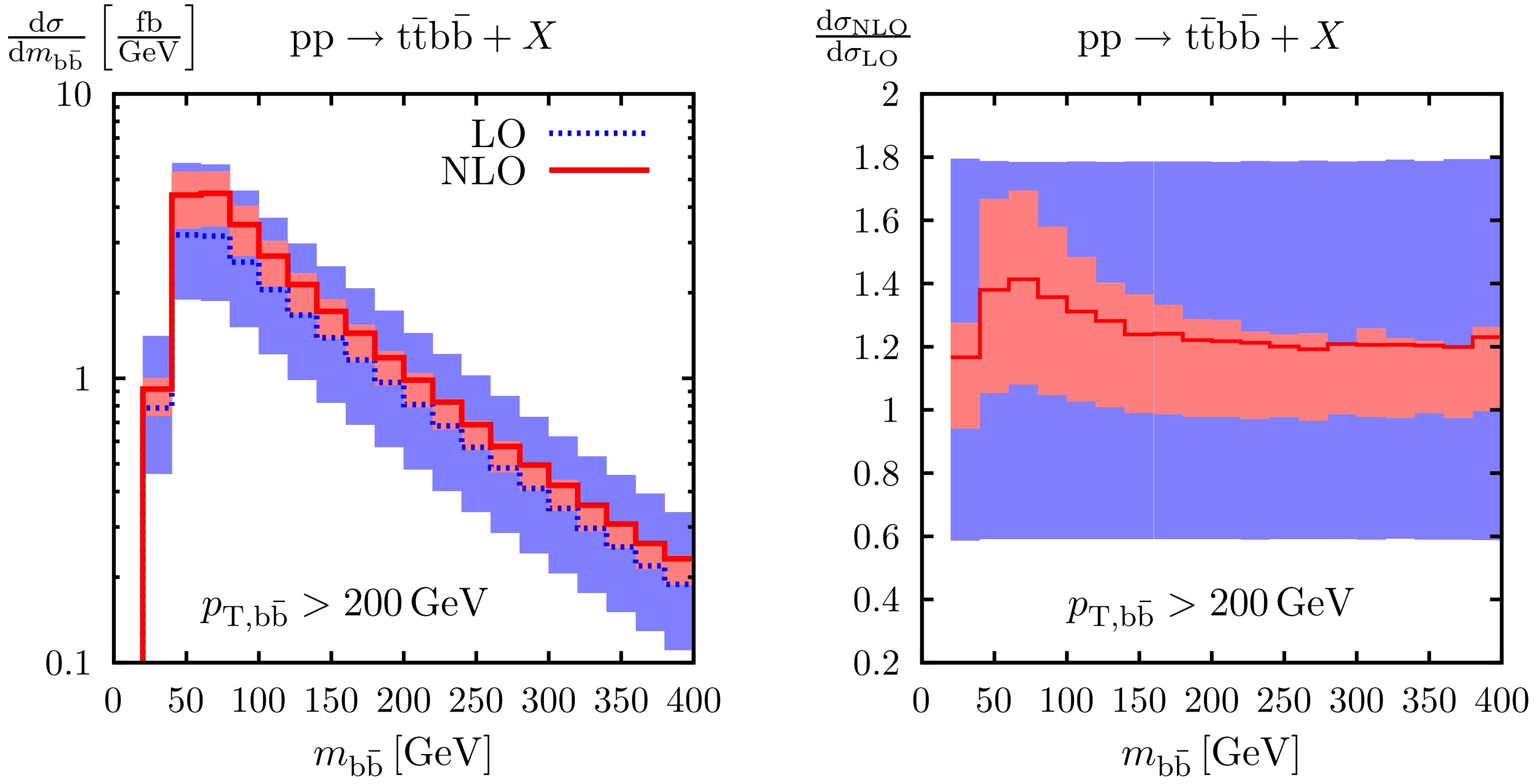

- small NLO correction $K \simeq 1.31$
- NLO corrections distort shape by about 20%
- NLO scale uncertainty $\sim 20\%$

Speed and precision of calculation

Runtime and statistical precision with 3 GHz Intel Xeon processor

	$\sigma/\sigma_{\mathrm{LO}}$	# events (after cuts)	$(\Delta\sigma)_{\mathrm{stat}}/\sigma$	runtime	time/event
tree level	86%	5.3×10^6	0.4×10^{-3}	38 min	0.4 ms
virtual	−11%	0.26×10^6	0.6×10^{-3}	13 h	180 ms
real + dipoles	49%	10×10^6	3×10^{-3}	40 h	14 ms
total	124%		4×10^{-3}	53 h	

- 2 CPU days $\Rightarrow$ $\mathcal{O}(10^7)$ events and $\mathcal{O}(10^{-3})$ statistical uncertainty for σ_{tot} (distributions obtained with $\sim 5 \times 10^8$ events after cuts)
- speed of virtual corrections remarkably high: $180\,\mathrm{ms/event}$ (including colour and polarizations sums)
- for same precision ($\Delta\sigma/\sigma$) virtual corrections require less CPU-time than real corrections (scale-dependent statement!)

Conclusions

Feynman diagram approach

- works very well for processes with up to 6 external particles
- remarkably high CPU speed
- very good perspectives to study other six-particle processes

NLO QCD calculation for $\mathrm{pp} \to \mathrm{t\bar{t}b\bar{b}} + X$ at the LHC

- very important for $\mathrm{t\bar{t}H}$ measurement at LHC
- calculation performed by two different groups with completely different methods
  agreement at per-mille level

QCD scale used by ATLAS not adequate $\Rightarrow$ replaced by new scale

- stabilizes QCD prediction: $K = 1.8 \pm 34\% \Rightarrow K = 1.25 \pm 21\%$
- cross section by factor 2 larger as assumed in ATLAS studies

Backup slides

4-dimensional identities

- Chisholm identity

$$\gamma^\alpha\gamma^\beta\gamma^\gamma = g^{\alpha\beta}\gamma^\gamma - g^{\alpha\gamma}\gamma^\beta + g^{\beta\gamma}\gamma^\alpha + \mathrm{i}\epsilon^{\alpha\beta\gamma\delta}\gamma_\delta\gamma_5$$

$\Rightarrow$ eliminate $\gamma^\alpha\gamma^\beta\gamma^\gamma$ or $\epsilon^{\alpha\beta\gamma\delta}\gamma_\delta\gamma_5$ terms

consequences — Denner, Dittmaier, Roth, Wieders '05

$$\begin{aligned}\gamma^\mu\gamma^\alpha\gamma^\beta\omega_\pm\otimes\gamma_\mu\omega_\pm &= \gamma_\mu\omega_\pm\otimes\gamma_\mu\gamma^\beta\gamma^\alpha\omega_\pm\\ \gamma^\mu\gamma^\alpha\gamma^\beta\omega_\pm\otimes\gamma_\mu\omega_\mp &= \gamma_\mu\omega_\pm\otimes\gamma^\alpha\gamma^\beta\gamma_\mu\omega_\mp\end{aligned}$$

Sirlin '81

$$\begin{aligned}\gamma^\mu\gamma^\alpha\gamma^\nu\omega_\pm\otimes\gamma_\mu\gamma^\beta\gamma_\nu\omega_\pm &= 4g^{\alpha\beta}\gamma^\mu\omega_\pm\otimes\gamma_\mu\omega_\pm\\ \gamma^\mu\gamma^\alpha\gamma^\nu\omega_\pm\otimes\gamma_\mu\gamma^\beta\gamma_\nu\omega_\mp &= 4\gamma^\beta\omega_\pm\otimes\gamma^\alpha\omega_\mp\end{aligned}$$

$\Rightarrow$ simplify contracted Dirac chains

- Schouten identity

$$\epsilon_{[\alpha\beta\gamma\delta}\,g_{\mu]\nu} = \epsilon_{\alpha\beta\gamma\delta}\,g_{\mu\nu} + \epsilon_{\beta\gamma\delta\mu}\,g_{\alpha\nu} + \epsilon_{\gamma\delta\mu\alpha}\,g_{\beta\nu} + \epsilon_{\delta\mu\alpha\beta}\,g_{\gamma\nu} + \epsilon_{\mu\alpha\beta\gamma}\,g_{\delta\nu} = 0$$

- products of ϵ tensors are eliminated via

$$\epsilon^{\alpha\beta\gamma\delta}\epsilon^{\mu\nu\rho\sigma} = -\begin{vmatrix} g^{\alpha\mu} & g^{\alpha\nu} & g^{\alpha\rho} & g^{\alpha\sigma}\\ g^{\beta\mu} & g^{\beta\nu} & g^{\beta\rho} & g^{\beta\sigma}\\ g^{\gamma\mu} & g^{\gamma\nu} & g^{\gamma\rho} & g^{\gamma\sigma}\\ g^{\delta\mu} & g^{\delta\nu} & g^{\delta\rho} & g^{\delta\sigma}\end{vmatrix}$$

4-dimensional identities (cont.)

- decomposition of metric tensor

$$g^{\mu\nu} = \sum_{i,j=0}^{3} g^{ij}\, n_i^\mu\, n_j^\nu$$

in terms of four independent orthonormal four-vectors n_j^μ
with $n_i^\mu\, n_{j,\mu} = g_{ij}, \quad g_{ij} = g^{ij} = \mathrm{diag}(1,-1,-1,-1)$
n_i^μ can be constructed from three linearly-independent massless momenta p_i, p_j, p_k

$$n_0^\mu(p_i,p_j,p_k) = \frac{1}{\sqrt{2\,(p_i p_j)}}\left(p_i^\mu + p_j^\mu\right), \qquad n_1^\mu(p_i,p_j,p_k) = \frac{1}{\sqrt{2\,(p_i p_j)}}\left(p_i^\mu - p_j^\mu\right)$$

$$n_2^\mu(p_i,p_j,p_k) = -\frac{1}{\sqrt{2\,(p_i p_j)\,(p_i p_k)\,(p_j p_k)}}\left[(p_j p_k)\,p_i^\mu + (p_i p_k)\,p_j^\mu - (p_i p_j)\,p_k^\mu\right]$$

$$n_3^\mu(p_i,p_j,p_k) = -\frac{1}{\sqrt{2\,(p_i p_j)\,(p_i p_k)\,(p_j p_k)}}\,\epsilon^{\mu\alpha\beta\gamma}\,p_{i,\alpha}\,p_{j,\beta}\,p_{k,\gamma}$$

no complicated denominators

$\Rightarrow$ decoupling of spinor chains or other objects $\quad \bar{v}_1\gamma^\mu u_2\ \bar{v}_3\gamma_\mu u_4 = \sum_{i,j=0}^{3} \bar{v}_1 \not{n}_i u_2\ \bar{v}_3 \not{n}_j u_4$

Standard matrix elements for $\bar{q}q \to t\bar{t}b\bar{b}$

25 types of standard matrix elements (polarization dependent)

- 10 of "massless" type: one Dirac matrix per chain

$$\bar{v}(p_1)\not{p}_i\omega_\alpha u(p_2)\ \bar{v}(p_3)\gamma^\mu\omega_\beta u(p_4)\ \bar{v}(p_5)\gamma^\mu\omega_\rho u(p_6)$$

$$\bar{v}(p_1)\not{p}_i\omega_\alpha u(p_2)\ \bar{v}(p_3)\not{p}_j\omega_\beta u(p_4)\ \bar{v}(p_5)\not{p}_k\omega_\rho u(p_6)$$

- 15 of "massive" type: 2/0 Dirac matrices inside the $t\bar{t}$ chain*

$$\bar{v}(p_1)\not{p}_i\omega_\alpha u(p_2)\ \bar{v}(p_3)\not{p}_j\gamma^\mu\omega_\beta u(p_4)\ \bar{v}(p_5)\not{p}_k\omega_\rho u(p_6)$$

$$\bar{v}(p_1)\gamma^\mu\omega_\alpha u(p_2)\ \bar{v}(p_3)\not{p}_j\not{p}_j\omega_\beta u(p_4)\ \bar{v}(p_5)\gamma^\mu\omega_\rho u(p_6)$$

$$\bar{v}(p_1)\gamma^\mu\omega_\alpha u(p_2)\ \bar{v}(p_3)\gamma^\mu\gamma^\nu\omega_\beta u(p_4)\ \bar{v}(p_5)\gamma^\nu\omega_\rho u(p_6)$$

$$\bar{v}(p_1)\gamma^\mu\omega_\alpha u(p_2)\ \bar{v}(p_3)\omega_\beta u(p_4)\ \bar{v}(p_5)\gamma^\mu\omega_\rho u(p_6)$$

$$\bar{v}(p_1)\not{p}_i\omega_\alpha u(p_2)\ \bar{v}(p_3)\omega_\beta u(p_4)\ \bar{v}(p_5)\not{p}_k\omega_\rho u(p_6)$$

*price to pay for the presence of massive top quarks

Set-up for numerical calculation of $\mathrm{pp} \to \mathrm{t\bar{t}b\bar{b}} + X$

Parton masses

- top mass: $m_\mathrm{t} = 172.6\,\mathrm{GeV}$
- bottom mass: $m_\mathrm{b} = 0\,\mathrm{GeV}$ (massless approximation better than 3% at LO)

jet definition: k_T algorithm as used at Tevatron run II Blazey et al. '00

- select massless partons (g, q and b) with $|\eta| < 5$
- reconstruct jets with $\sqrt{\Delta\phi^2 + \Delta y^2} > D = 0.4$

cuts for b jets: (motivated by $\mathrm{t\bar{t}H}$ analysis)

- require two b-jets with $p_{\mathrm{T},j} > 20\,\mathrm{GeV}$ and $y_j < 2.5$ (b tagging!)
- $\mathrm{b\bar{b}}$ invariant mass: $m_{\mathrm{b\bar{b}}} > m_{\mathrm{b\bar{b}},\mathrm{cut}} = 100\,\mathrm{GeV}$
- top quarks fully inclusive (no decays and no cuts)

NLO settings: [LO obtained with LO α_S, LO PDFs and 1-loop running]

- central scale: $\mu_0 = m_\mathrm{t} + m_{\mathrm{b\bar{b}},\mathrm{cut}}/2 \quad \Rightarrow \quad \mu_0^2 = m_\mathrm{t}\sqrt{p_{\mathrm{T,b}}\,p_{\mathrm{T},\bar{\mathrm{b}}}}$
- factor-2 scale variations to estimate LO and NLO scale uncertainty
- PDFs: CTEQ6M with $\alpha_\mathrm{S}(M_\mathrm{Z}) = 0.118$

Effect of a jet veto for $\mathrm{pp} \to \mathrm{t\bar{t}b\bar{b}} + X$

Jet veto could reduce large $\mathrm{t\bar{t}b\bar{b}}$ background

Bredenstein, Denner, Dittmaier, Pozzorini

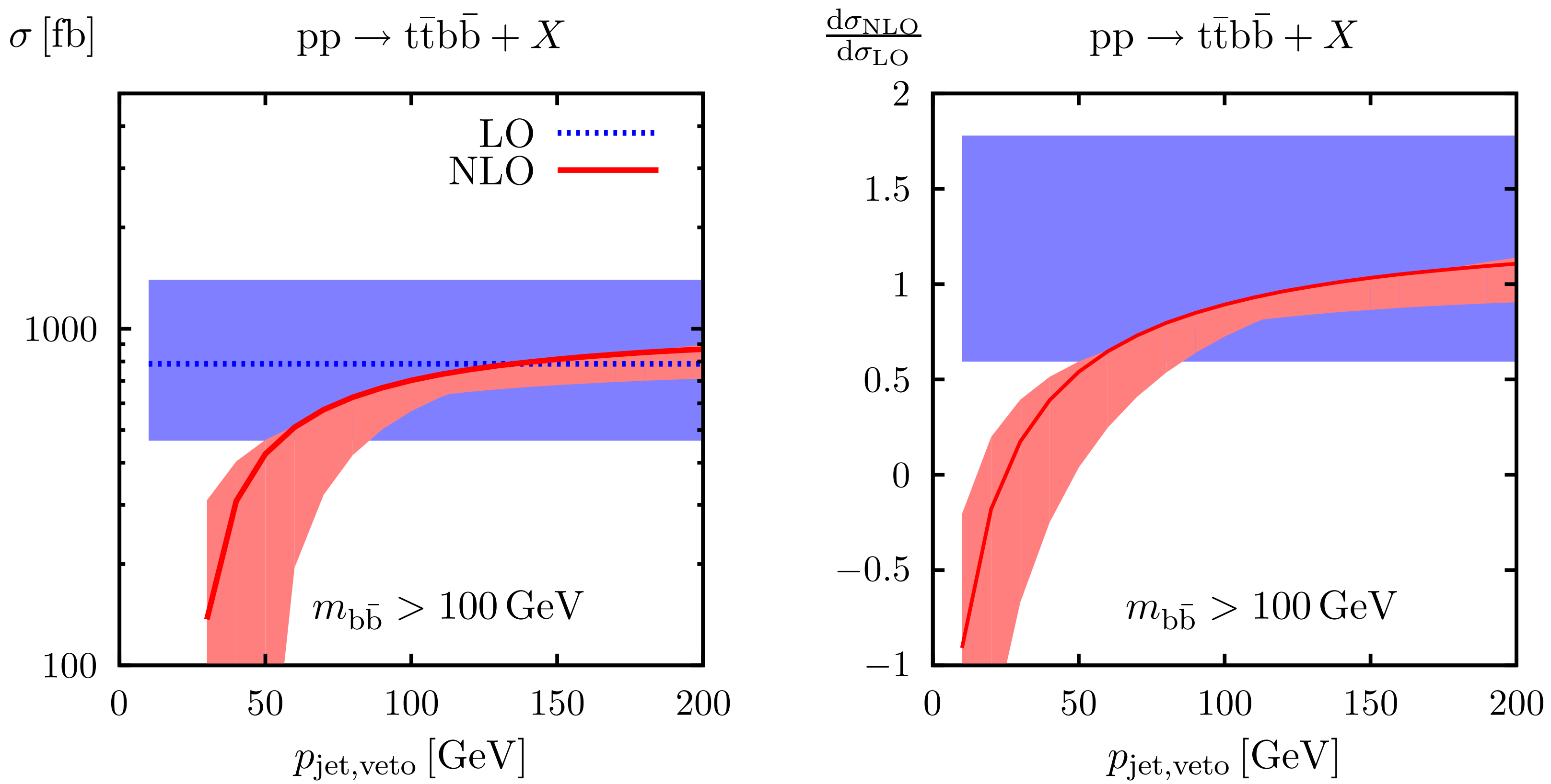

- perturbative instability for small $p_{\mathrm{jet,veto}}$ ($\lesssim 50\,\mathrm{GeV}$)
- safe jet-veto values $p_{\mathrm{jet,veto}} \sim 100\,\mathrm{GeV}$ ($\Rightarrow$ 30% reduction in cross section)
  - K factor reduced from $K = 1.24$ to $K \simeq 0.9$
  - NLO scale uncertainty hardly affected ($\sim 19\%$)